Synthesis of Polymandelide: A Degradable Polylactide Derivative with Polystyrene-like Properties

Tianqi Liu,[†] Tara L. Simmons,[†] David A. Bohnsack,[‡] Michael E. Mackay,[‡] Milton R. Smith, III,[†] and Gregory L. Baker*[,†]

Department of Chemistry, Michigan State University, East Lansing, Michigan 48824, and Department of Chemical Engineering and Materials Science, Michigan State University, East Lansing, Michigan 48824-1226

Received August 11, 2006; Revised Manuscript Received June 12, 2007

ABSTRACT: Polymandelide, an aryl analogue of polylactide, was synthesized by the ring-opening polymerization of mandelide, the cyclic dimer of mandelic acid. The poor solubility of *rac*-mandelide limited the synthesis of polymandelide via solution polymerization, but polymerization of mandelide at 70 °C as a heterogeneous slurry in acetonitrile yielded first-order kinetic plots and polydispersities <1.2. High molecular weight polymer prepared by melt polymerizations at $T > 150$ °C exhibit properties that mimic those of polystyrene. Polymandelide is a glassy amorphous polymer with a T_g of 100 °C, with rheological properties comparable to polystyrene, and thermal gravimetric analyses under nitrogen show that the polymer is stable to ∼300 °C. Racemization during polymerization precluded formation of a crystalline polymer. Degradation of polymandelide in pH 7.4 buffer at 55 °C is consistent with a bulk erosion model and, due to its high T_g, proceeds at ∼1/100 the rate of polylactide under similar conditions.

Introduction

From an environmental perspective, degradable polymers based on renewable resources are attractive alternatives to materials derived from petroleum. Poly(hydroxybutyrate)s and poly(lactide)[1−4] are among the most widely studied degradable polymer systems, and polylactide is now commercialized as a commodity polymer for high volume applications such as fibers and packaging materials.[5] While a broad range of physical properties is available from these two polymer families, a glassy, amorphous, degradable polymer with a high glass transition temperature (T_g) is unavailable. The backbone of polylactide is relatively flexible, resulting in T_gs ranging from 30 to 60 °C, depending on the degree of crystallinity and molecular weight of the polymer. Since adding bulky groups to the polymer backbone should increase rotational barriers along the polymer backbone and increase T_g, we initially synthesized poly(phenyllactide),[6] an aromatic derivative of polylactide. The disappointingly low T_g of 50 °C for poly(phenyllactide) can be explained by the flexible methylene group that links the ring to the polymer backbone. Removing the methylene and substituting an aromatic ring for the methyl group of polylactide should, by analogy to the structure of polystyrene, result in a polymer with a significantly higher T_g. Thus, mandelide, the dimer of mandelic acid (2-hydroxyphenylacetic acid), is a particularly intriguing monomer for ring-opening polymerization. In this report, we describe the preparation of high molecular weight polymandelide, a polymer that shares many of the physical properties of polystyrene, but with the added feature of being degradable.

Prior to our work, several groups explored the preparation of the mandelic acid homopolymer, but the schemes reported to date resulted in polymers with number-average molecular weights <5000, too low for most practical applications. Probably due to their low molecular weights, no glass transition temperatures were reported for these polymers. Direct condensation of α-bromophenylacetic acid in the presence of triethylamine,[7] transesterification of methyl mandelate,[8] and condensation of mandelic acid all provided low molecular weight polymers with degrees of polymerization near 20. Several indirect routes to polymandelide also have been reported. In perhaps the earliest synthesis of the homopolymer of mandelic acid, the trimethyltin ester of α-bromophenylacetic acid was pyrolyzed, and the resulting viscous solid was identified as polymandelide.[9] Deoxypolymerization of phenylglyoxalic acid using cyclic phosphites yielded oligomers,[10] and ring-opening polymerization (with loss of CO_2) of the anhydridocarboxylate of mandelic acid gave polymandelide with degrees of polymerization as high as 30.[11] The latter method proceeds at room temperature and is claimed to proceed with retention of configuration, although crystalline polymers were not formed.

A series of articles reported the preparation and degradability of low molecular weight mandelic acid copolymers (M_n < 2000) by the direct condensation of L-lactic acid and DL-mandelic acid.[12−16] These copolymers covered the entire compositional range from 0 to 100% mandelic acid and were evaluated as potential drug carriers. Lactic acid-based poly(ester−urethane)s have been reported that contain up to 20 mol % DL-mandelic acid in low molecular weight poly(lactic acid) segments.[17,18] Increasing the mandelic acid content increased the T_g of the lactide segment.[18]

Polylactides are easily prepared by the ring-opening polymerization of lactide,[19] the cyclic dimer of lactic acid, and ring-opening polymerization would seem the logical route to high molecular weight polymandelide. However, polymerization of mandelide to high molecular weight homopolymers poses significant challenges. Syntheses of high molecular weight substituted polylactides[20−22] often present problems related to the increased steric demands of substituted glycolides. In addition, monomer purification can be difficult, especially when glycolides contain polar functional groups. Because the mandelide ring is more sterically hindered than lactide, the rate of ring-opening polymerization should be slower, and one might

[†] Department of Chemistry.
[‡] Department of Chemical Engineering and Materials Science.

10.1021/ma061839n CCC: $37.00
Published on Web 07/31/2007

Scheme 1

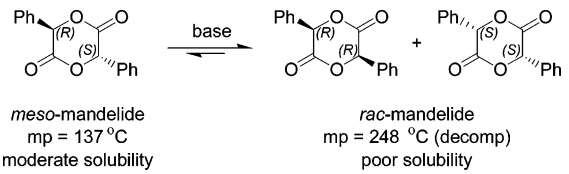

expect that the equilibrium nature of lactide polymerizations[23,24] could limit mandelide polymerizations to low conversions and low molecular weights. Solution polymerizations are hampered by the poor solubility of mandelides in many organic solvents. Furthermore, melt polymerizations also have unfavorable characteristics. For instance, *rac*-mandelide (an equimolar mixture of *R*,*R* and *S*,*S* enantiomers) decomposes on melting (Scheme 1). While the *meso* isomer (*R*,*S*), melting at 137 °C, would appear amenable to melt polymerization techniques, the methine protons of the mandelide ring are particularly labile under basic conditions[25] since they are α to an aromatic ring, a carbonyl, and an oxygen atom. Consequently, *meso*-mandelide rapidly epimerizes to the higher melting *rac* isomers. Despite these challenges, the prospect of a glassy degradable polymer with polystyrene-like properties makes polymandelide an attractive synthetic target.

Experimental Section

Unless otherwise specified, ACS reagent grade starting materials were used as received from Aldrich. THF was refluxed over CaH_2 and then was distilled from sodium benzophenone ketyl under nitrogen. Toluene was freshly distilled from sodium benzophenone ketyl under nitrogen. ^{1}H NMR (300 MHz) and ^{13}C NMR (125 MHz) analyses were performed at room temperature in DMSO-d_6 on a Varian Gemini-300 spectrometer using TMS as the chemical shift standard. Polymer molecular weights were measured by gel permeation chromatography (GPC) at 35 °C in THF using a PLgel 20 μm MIXED-B column at a flow rate of 1 mL/min. Two detectors were used: a Waters R410 differential refractometer and a Waters 996 photodiode array. The concentration of the polymer samples was 1 mg/mL, and each solution was filtered through a Whatman 0.2 μm PTFE filter before injection. Molecular weights are reported relative to monodisperse polystyrene standards. Differential scanning calorimetry (DSC) data were obtained with a Perkin-Elmer DSC 7 instrument calibrated with indium and hexyl bromide standards. The samples were sealed in aluminum pans and were heated at 10 °C/min under a helium atmosphere. Liquid nitrogen was used as the coolant. Thermogravimetric analysis (TGA) data were obtained from a Perkin-Elmer TGA 7 instrument at a heating rate of 40 °C/min under nitrogen. Reported melting points were measured with an Electrothermal melting point apparatus and are uncorrected. The densities of solutions were measured using a series of hydrometers (Curtin Matheson Scientific, Inc.).

Synthesis of *rac*- and *meso*-Mandelide. Racemic mandelic acid (6.03 g, 39.7 mmol) and a catalytic amount of *p*-toluenesulfonic acid (0.20 g, 1.2 mmol) were dissolved in mixed xylenes (600 mL). The solution was refluxed for 3 days, and water was removed via a Dean−Stark trap. The conversion of the reaction was monitored by NMR and by the amount of water that collected in the trap. Typically, the yield of the cyclized product reached a maximum at ∼3 days. The solution was allowed to cool to room temperature, and most of the *rac*-mandelide precipitated from solution. The solid was collected by filtration to give 1.3 g of *rac*-mandelide (47%, mp 193 °C (decomp), lit. 248−249 °C (decomp)[26]). ^{1}H NMR: δ 6.61 (s, 1H), 7.35−7.58 (m, 5H). ^{13}C NMR: δ 166.47, 132.32, 129.28, 128.35, 128.29, 77.47.

The filtrate was washed three times with saturated aqueous $NaHCO_3$, and the solvent was dried and removed by rotary evaporation. The resulting crude *meso*-mandelide was recrystallized three times from ethyl acetate to give 1.5 g (53%) of *meso*-mandelide, mp 137 °C. The *meso* isomer could also be purified, albeit in lower yield, by passing the crude filtrate through a layer of silica gel, followed by solvent removal and recrystallization. ^{1}H NMR: δ 6.44 (s, 1H), 7.35−7.62 (m, 5H). ^{13}C NMR: δ 164.71, 133.23, 129.56, 128.94, 127.56, 77.56.

Melt Polymerization of Mandelide. Stock solutions of Sn(2-ethylhexanoate)$_2$ and *tert*-butyl benzyl alcohol (BBA) in anhydrous toluene were prepared in a drybox and transferred to a Schlenk flask. The flask was then fitted with a vacuum adapter and removed from the box. Mandelide, previously dried overnight under reduced pressure (5 mTorr, 30 °C), was loaded into small glass ampules (∼3 mL) with stir bars and connected via a Cajon fitting to a T-shaped vacuum adapter fitted with a stopcock and an air-free Teflon valve. The apparatus was attached to a vacuum line and evacuated through the stopcock for 2 h. Then the ampule was backfilled with argon, and a syringe was used to add a predetermined amount of the Sn(2-ethylhexanoate)$_2$ and BBA solutions to the ampules though the air-free valve. After removing the solvent under vacuum, the glass ampules were sealed under vacuum. The ampules were added to a thermostatted silicon oil bath (typically 160 °C), and after desired time intervals, ampules were removed from the bath and the polymerizations were quenched in ice water. The ampules were then broken, and the residue was extracted with methylene chloride or THF. Filtration and removal of the solvent in vacuo gave a mixture of crude polymandelide and residual monomer as an off-white or light brown solid. The conversion of monomer to polymer was measured by ^{1}H NMR by integrating the methine proton signals from the monomer δ6.44 (*meso*) and 6.61 ppm (*rac*) and polymer (6.0−6.26 ppm). The residual monomer composition was determined by integration of the methine protons at δ6.44 (*meso*) and 6.61 ppm (*rac*).

Polymer Purification. Crude polymandelide was dissolved in methylene chloride, and the insoluble portion (*rac*-mandelide) was removed by filtration. The polymer solution was concentrated to ∼10 wt % and added dropwise to a stirring solution of cold methanol. The polymer precipitate was collected on a fritted glass funnel and dried under vacuum at 60−70 °C. If necessary, the precipitation procedure was repeated. When polymerizations were run to <80% conversion, purification was complicated by residual *rac*-mandelide that coprecipitates with the polymer. Monomer-free polymandelide was recovered in >80% yield by dissolving the polymer in a minimal amount of CH_2Cl_2, filtering to remove the less soluble *rac*-mandelide, and precipitating into cold methanol. The precipitated polymer was dried under vacuum at 60−90 °C until constant weight was obtained, and NMR analyses confirmed that the isolated polymandelide was free of monomer. Catalyst residues in polymandelide samples used for thermal analysis experiments were removed by dissolving the polymer in methylene chloride or toluene. After washing with dilute HCl, the organic layer was washed with distilled water until the water layer was neutral, and the resulting solution was precipitated into cold methanol to afford white polymer. GPC analysis of the polymer before and after the extractions showed no change in molecular weight.

Solution Polymerizations. Mandelide (2.50 g, 9.32 mmol, *meso*:*rac* = 3:1) was placed in a Schlenk flask and dried under vacuum. After transferring the flask into a drybox, anhydrous acetonitrile (10 mL, water <0.001% (Aldrich)) was added to the flask. The flask was then connected to a vacuum line and heated to 70 °C under argon. Sn(2-ethylhexanoate)$_2$ (93.2 μmol) and BBA (93.2 μmol) solutions were added to the flask via syringe under argon to initiate polymerization. At predetermined intervals, aliquots of the reaction solution were removed via syringe and analyzed by NMR and GPC to determine the conversion and polymer molecular weights. Conversion was calculated by integrating of the methine proton signals from the monomer and polymer. The residual monomer composition was determined by integration of the methine protons at δ6.44 (*meso*) and 6.61 ppm (*rac*).

Density Measurements. Polymandelide powder obtained from precipitation of the polymer was melt-pressed at 140 °C using a Carver press at 20 000 psi. Chunks of polymer that were free of

Scheme 2. Synthesis of Polymandelide via Ring-Opening Polymerization

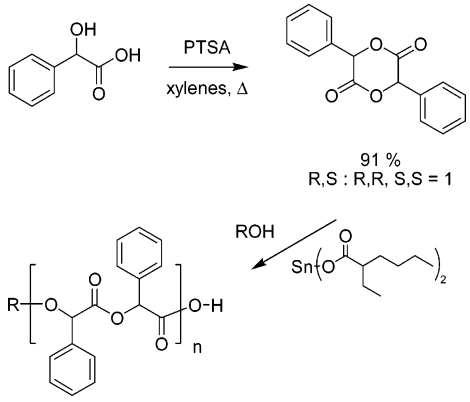

air bubbles were selected for density measurements. Samples were added to a graduated cylinder filled with distilled water at 25 °C, and the density was gradually increased by adding NaCl until polymandelide samples remained suspended in the solution. Once the salt solution had fully equilibrated, the density of the solution (equivalent to the density of the polymer) was measured by a hydrometer.

Rheolgical Measurements. The viscoelastic properties of the polymer were characterized with an Rheometrics ARES rheometer using 8 mm diameter parallel plates to determine the storage (G') and loss (G'') moduli. All experiments were performed in the linear viscoelastic region, and temperatures from 150 to 200 °C were used and results shifted to a reference temperature of 170 °C. The plateau modulus (G_N^0) was determined by equating the storage modulus to its value at the frequency corresponding to the minimum in the loss angle,[27] and the terminal viscosity (μ_0) was determined by extrapolation.

Hydrolytic Degradation of Polymandelide. A pH 7.4 phosphate buffer solution was prepared by adding a dilute NaOH solution to a commercially available phosphate buffer (pH = 7.0) at 55 °C. Multiple samples were prepared by adding ~50 mg of polymer particles (~1 mm in diameter) to test tubes with screw caps. After adding 15 mL of pH 7.4 phosphate buffer solution, the tubes were sealed and placed into a water/ethylene glycol bath thermostatted at 55 ± 0.2 °C. At desired times, the test tubes were removed from the bath. The solutions were then filtered through a tared, fritted glass funnel, and the collected polymer powder was rinsed repeatedly with a large amount of distilled water. The polymer and the funnel were dried under vacuum at 70 °C until constant weight was obtained. Dried samples were analyzed by GPC.

Results and Discussion

Bulk Polymerization of Mandelide. As shown in Scheme 2, we used a modified literature procedure to prepare the *meso* and *rac* diastereomers of mandelide. The acid-catalyzed dimerization of mandelic acid[26] yielded a statistical mixture of the *rac* and *meso* diastereomers. On cooling the reaction solution to room temperature, the less soluble *rac*-mandelide precipitated from solution and was isolated in (~45% yield). *meso*-Mandelide (45%) was isolated from the filtrate and purified by crystallization from ethyl acetate. Our initial emphasis was on melt polymerizations of the *meso* isomer because both mandelides have poor solubilities and *rac*-mandelide decomposes on melting. Later we found that mandelide's high racemization rate under polymerization conditions makes isolation of pure *rac*- and *meso*-mandelide unnecessary.

Entries 1−4 in Table 1 show typical data for the polymerization of purified *R,S*-mandelide. Melt polymerizations were run in sealed ampules at 160 °C using Sn(2-ethylhexanoate)$_2$ as the catalyst and 4-*tert*-butylbenzyl alcohol as the initiator. Our initial polymerizations went to high conversion, but the molecular weights were about half those expected from the monomer-to-initiator ratios used in the polymerizations (entry 1), suggesting that water or a similar impurity was acting as an adventitious initiator for a large fraction of the chains. Higher molecular weight samples (above the chain entanglement limit) were needed for reliable T_g measurements. Attempts to remove impurities by recrystallization were unsuccessful, but recrystallization followed by drying the monomer under more rigorous conditions (5 mTorr at 30 °C for 48 h) provided polymers with molecular weights that nearly match those predicted by the monomer/initiator ratio (entry 2). In addition, the molecular weight distributions were narrow (<1.3), reflecting controlled polymerization. A more aggressive drying protocol, 10^{-5} Torr at 30−45 °C (entries 3 and 4), did not provide further improvement in molecular weights or polydispersity. At a monomer-to-catalyst ratio of 500:1 and without added 4-*tert*-butylbenzyl alcohol (entry 5) mandelide polymerized more slowly (70% conversion at 1 h, 68 000 g/mol), suggesting a low level of adventitious initiator remained in the monomer. A large-scale melt polymerization reaction (128 g) run in a drybox gave similar results.

Table 1. Melt Ring-Opening Polymerization of *R,S*-Mandelide

entry	[M]/[I]	time (min)	% conv[a]	M_n(theor)[b]	M_n[c]	PDI
1[d]	50	3	93	12 500	6 840	1.17
2[d]	50	3	86	11 500	10 400	1.19
3[d]	50	4	91	12 060	11 480	1.26
4[d]	50	4	97	12 950	11 430	1.29
5[e]		60	73		68 300[f]	1.63
6[g]		60	74		80 100	1.84

[a] Measured by ^{1}H NMR. [b] Corrected for conversion. [c] Measured by GPC in THF using polystyrene standards for calibration. [d] Polymerized in a sealed tube at 160 °C using 4-*tert*-butylbenzyl alcohol as initiator. [e] A 3:1 mixture of *R,S*- and *R,R/S,S*-mandelide was polymerized with no added initiator in a sealed tube at 150−160 °C; [M]/[catalyst] = 500. [f] M_w determined by light scattering in THF was 137 000 g/mol. [g] A 3:1 mixture of *R,S* and *R,R/S,S* was polymerized on a 120 g scale in a drybox; [M]/[catalyst] = 500.

The products of these polymerizations are glassy, amorphous materials that share many of the same properties as polystyrene. The NMR spectra in the methine (^{1}H and ^{13}C) and carbonyl regions (^{13}C) consist of a complicated pattern of resonances (see Figure S-1 and Figure S-2, Supporting Information). The stereosequences have not been assigned, but the large number of peaks suggests a high degree of stereochemical disorder. Consistent with the NMR data, characterization of polymandelide by DSC and wide-angle X-ray diffraction showed no signs of crystallinity, even after annealing samples at 130 °C overnight. Monomer epimerization during polymerization also contributed to the irregular tacticity of polymandelide. Samples from a melt polymerization at 50% conversion were analyzed by ^{1}H NMR, and the spectra showed that the monomer pool had racemized into a statistical mixture of diastereomers.[28] Since typical mandelide polymerizations reach >90% conversion, *rac*-mandelide units almost certainly copolymerize with *meso*-lactide.

We are aware of one report of a polymandelide T_g, ~75 °C for polymandelide with M_n ~ 1100 g/mol.[12] As expected, data from various mandelide polymerizations show that T_g increases with molecular weight, from ~95° for M_n = 16 000 g/mol (PDI = 1.33) to 100 °C when M_n = 68 000 g/mol (PDI = 1.63). In addition to having a T_g similar to that of polystyrene (T_g = 109 °C), polymandelide and polystyrene form clear, colorless films by casting from solution or compression molding. While the ester makes polymandelide more polar than polystyrene (calculated solubility parameter for polymandelide = 10.4 vs 9.05

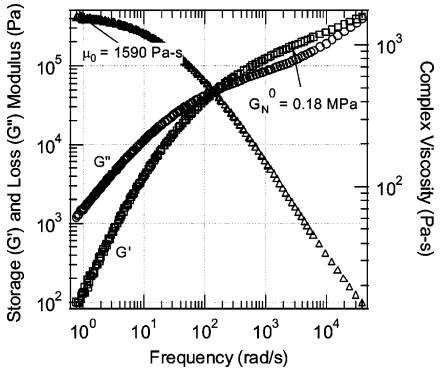

Figure 1. Linear viscoelastic properties of polymandelide at 170 °C (M_w = 50 000 g/mol).

$(cal/cm^3)^{1/2}$ for polystyrene), both dissolve in common organic solvents such as toluene, chloroform, THF, ethyl acetate, and acetone. Nonsolvents include hexanes, ether, and methanol. Flotation measurements indicate that polymandelide is more dense than polystyrene, ρ = 1.25 vs 1.05 g/cm^3.

We characterized the rheological properties of a polymandelide sample with M_w = 50 000 g/mol. The terminal viscosity and storage modulus were found to be remarkably similar to those of polystyrene. The data of Fox and Flory[29,30] were used to find the terminal viscosity at 170 °C using the equation

$$292\ \text{Pa·s} \times [M_w/32.7\ \text{kDa}]^{3.68}$$

where M_w is the weight-average molecular weight. The terminal viscosity of polymandelide is 1590 Pa·s while polystyrene of equivalent molecular weight has a terminal viscosity of 1390 Pa·s, showing good agreement. Furthermore, the plateau modulus, a good indicator of the molecular weight between entanglements, is equal to that for polystyrene,[31] suggesting the flow properties of this material are similar to those of polystyrene.

Solution Polymerization of Mandelide. Solution polymerization could offer advantages over melt polymerizations, such as slower, more controlled reactions and potential access to more complicated architectures such as block copolymers. Toluene, a common solvent for lactide polymerization, proved to be unsatisfactory for mandelide polymerization because of low monomer solubility. We elected to use acetonitrile for polymerizations because of higher monomer solubilities (1.5 mol/L at 50 °C for *meso*-mandelide, lower for *rac*-mandelide). ^{1}H NMR analysis of initial polymerizations showed that *meso*-mandelide was stereochemically labile in acetonitrile at 70 °C in the presence of a standard catalyst/initiator system, Sn(2-ethylhexanoate)$_2$/4-*tert*-butylbenzyl alcohol, and we were concerned that racemization would steadily increase the concentration of the poorly soluble *rac*-mandelide and lead to precipitation of *rac*-mandelide. Reasoning that rapid epimerization also would allow us to polymerize a *mixture* of the *meso* and *rac* diastereomers, we polymerized a mixture of mandelide diastereomers (*meso*:*rac* = 3:1) at 70 °C using Sn(2-ethylhexanoate)$_2$ as catalyst and 4-*tert*-butylbenzyl alcohol as initiator (Figure 2).

Monitoring the polymerization by ^{1}H NMR showed that the *meso/rac* mixture epimerized to a 1:1 mixture of *meso* and *rac* diastereomers within 30 min (< 20% conversion) which was maintained throughout the polymerization (see Figure S-3, Supporting Information). As the concentration of the poorly soluble *rac*-mandelide increased, it precipitated, and the polymerization mixture remained heterogeneous until the conversion reached ~60%. Presumably, at that point the polymerization had sufficiently depleted the monomer pool so that the *rac*-mandelide concentration was no longer over its solubility limit. Despite potential complications caused by epimerization and crystallization, the data shown in Figure 2 reveal first-order kinetics for the solution polymerization. In addition, the number-average molecular weight is linearly dependent on conversion and polydispersities approach 1.1 (Figure 3). These remarkable data likely reflect maintenance of a constant monomer concentration throughout the polymerization, controlled by the solubility of the monomer. These results also show that although polymerizations under these conditions do not allow the synthesis of stereoregular polymandelide, they exhibit "living" character like other substituted glycolide polymerizations. This opens possibilities for the preparation of more complicated architectures from mandelides, such as block copolymers, which will extend the parallels between polymandelide and polystyrene.

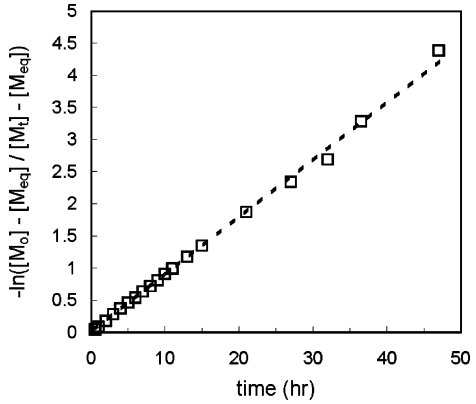

Figure 2. Kinetics of the solution polymerization of mandelide in CH_3CN at 70 °C under argon. [Mandelide]:[Sn(2-ethylhexanoate)$_2$]:[BBA] = 100:1:1; [mandelide] = 0.93 mol/L (75% *meso*-mandelide and 25% *rac*-mandelide). M_{eq} = 0.037 M.

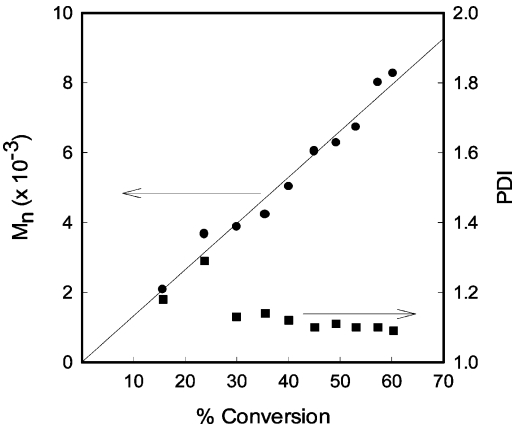

Figure 3. Evolution of M_n with conversion during the polymerization of mandelide in CH_3CN at 70 °C under argon. [Mandelide]:[Sn(2-ethylhexanoate)$_2$]:[BBA] = 100:1:1; [mandelide] = 0.93 mol/L (75% *meso*-mandelide and 25% *rac*-mandelide).

We briefly explored the synthesis of crystalline polymandelide via stereospecific polymerization of *meso*-mandelide at low temperatures, where racemization might be less severe. A stereoregular polymer derived from *meso*-mandelide would need a regular *RSRS* or *RRSS* pattern along the polymer backbone. In principle, this could be achieved using Coates' Zn β-diketiminate catalysts, which polymerize *meso*-lactide to syndiotactic polylactic acid,[32−35] or LiOtBu, shown by Bero et al. to polymerize *rac*-lactide to heterotactic poly(lactic acid).[36] We attempted to polymerize *meso*-mandelide in CH_2Cl_2 at room

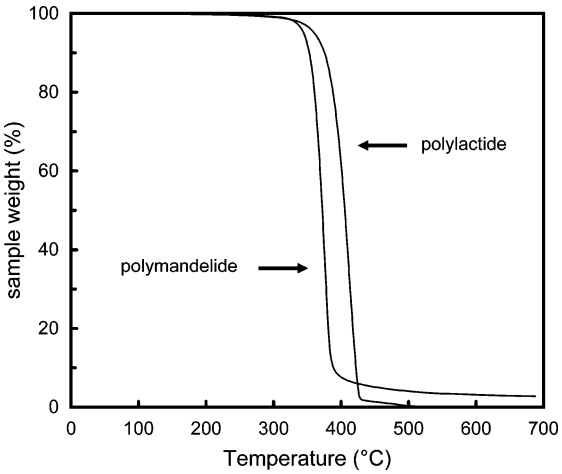

Figure 4. Thermal gravimetric analysis of polymandelide and polylactide after washing with dilute HCl. Samples were heated at 40 °C/min under N_2.

temperature using $[LZnOMe]_2$ as the catalyst, where L is 2-((2,6-diethylphenyl)amido)-4-((2,6-diethylphenyl)imino)-2-pentenato. *meso*-Mandelide was stereochemically stable to the reaction conditions but did not polymerize to any significant extent, possibly due to the increased steric demands of mandelide compared to lactide. At slightly elevated temperatures, racemerization was detected by ^{1}H NMR, and the concentration of *rac*-mandelide increased, and eventually the poorly soluble *rac* diastereomer precipitated from solution. ^{1}H NMR resonances for the conjugate acid of the diketiminate ligand were also detected, indicating extensive catalyst decomposition.[37] At this point, we abandoned our attempts to prepare stereoregular polymandelide.

Thermal Degradation of Mandelide. Thermogravimetric analysis of purified polymandelide run under N_2 (Figure 4) showed an onset for decomposition at 320 °C, followed by a rapid weight loss. Such profiles are often attributed to depolymerization. Since polymerization catalyst residues can effect depolymerization via generation of volatile cyclic dimers or oligomers, we dissolved the polymer in CH_2Cl_2 and washed the polymer solutions with dilute HCl. We repeated this process until the TGA degradation profile was constant and free of catalyst. The thermal profile for polylactide purified in the same way is shown for comparison. The lower degradation temperature for polymandelide seems inconsistent with a simple depolymerization mechanism where the limiting step is evolution of the monomer, since lactide is more volatile than mandelide. Instead, activation of the carbon α to the carbonyl by the aromatic ring likely explains the polymandelide's onset for degradation being lower than for polylactide. Smith and Tighe[11] reported an onset for decomposition of low molecular weight polymandelide at ∼205 °C and identified carbon monoxide and benzaldehyde as the principal decomposition products of their thermogravimetric experiment. To see whether a similar pathway might be operating in high molecular weight polymer, we sealed a rigorously purified polymandelide sample (no detectable residual monomer) in a glass ampule and heated the sample in a 200 °C oil bath for 24 h. NMR analysis of the sample showed no significant changes in chemical structure of the polymer and no formation of mandelide. However, GPC traces revealed decreases in molecular weight and a singlet in the ^{1}H NMR at 10.0 ppm (1.7% in intensity, relative to all methine protons) consistent with the formation of an aldehyde, presumably benzaldehyde. The GPC data and formation of benzaldehyde are both consistent with chain scission.

The results of the sealed tube experiment point to chain scission as the degradation pathway. Chuchani and co-workers have extensively studied unimolecular decompositions of α-hydroxyacids and ester, which may have relevance to polymandelide decomposition.[38−40] The lower degradation temperature of polymandelide relative to polylactide parallels the stabilities of mandelic and lactic acids in the gas phase. Both of these extrude aldehyde and CO as shown in Scheme 3, the acid via decarbonylation of a transient lactone intermediate. In the gas phase, lactic acid decarbonylates much more readily than the ester, methyl lactate. Thus, the acid form in Scheme 3 will dominate the degradation, if present. Since the polymers have been washed with water during purification, we expect that some water will be present. At 200 °C, ester hydrolysis would play two important roles: (i) chain scission provides a mechanism to account for the decrease in polymer molecular weight, and (ii) hydrolysis would generate carboxylic acid end groups, accelerating decomposition. Using activation parameters from gas-phase studies, the estimated gas-phase decomposition rate for polymandelide is 3.6×10^{-5} s^{-1} at 200 °C.[41] Assuming that the polymandelide contains 0.1 wt % H_2O and acid end groups arise by hydrolysis, ∼2 wt % benzaldehyde would form after 24 h at 200 °C if the gas phase and melt decomposition rates are similar. Thus, it is plausible that the aldehyde observed by ^{1}H NMR arises from such a decomposition mechanism.[42]

Hydrolytic Degradation. Polymandelide is more hydrophobic than polylactide, which should lead to a slower degradation rate in vivo. Consistent with this notion, previous investigations of low molecular weight polymandelide samples (1300 g/mol) showed no weight loss after 15 weeks aging in phosphate buffered solution at pH 7.2 and 37 °C.[12,13] We chose to study the degradation of polymandelide under conditions identical to those we previously used to characterize substituted polylactides[43] (phosphate buffered solution at pH 7.4 and 55 °C). There are two advantages of this protocol: the degradation rates of poly(L-lactide) in phosphate buffered solutions were shown to mirror those measured in vivo,[44,45] and carrying out the degradation at 55 °C allows for completion of the degradation

Scheme 3

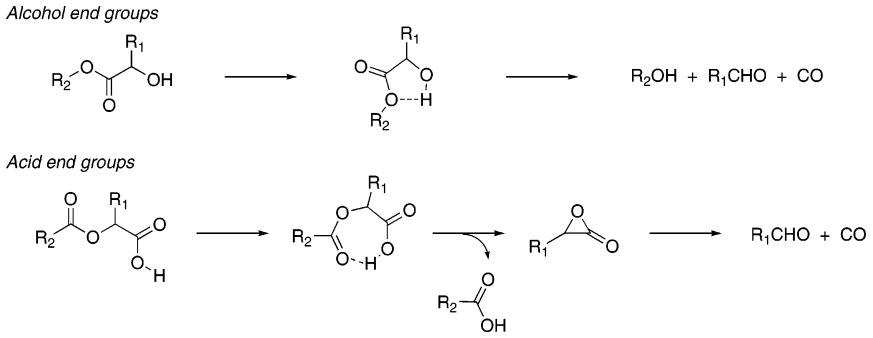

Table 2. Weight and Molecular Weight Change during Hydrolytic Degradation of Polymandelide in Phosphate Buffer (pH = 7.4) at 55 °C

degradation time (days)	wt % of remaining polymer	M_n[a]	PDI
0	100	78 200	1.61
12	96.0	73 800	1.62
20	96.4	66 860	1.64
40	98.6	58 900	1.67
64	96.1	49 100	1.67
91	92.4	33 800	1.80
161	78.3	13 300	2.48
188	62.8	6 980	4.19
225	51.2	4 590	4.84
304	26.2	*b*	*b*

[a] Measured by GPC in THF using polystyrene as the molecular weight standards. [b] The molecular weight distribution was too broad to be determined reliably.

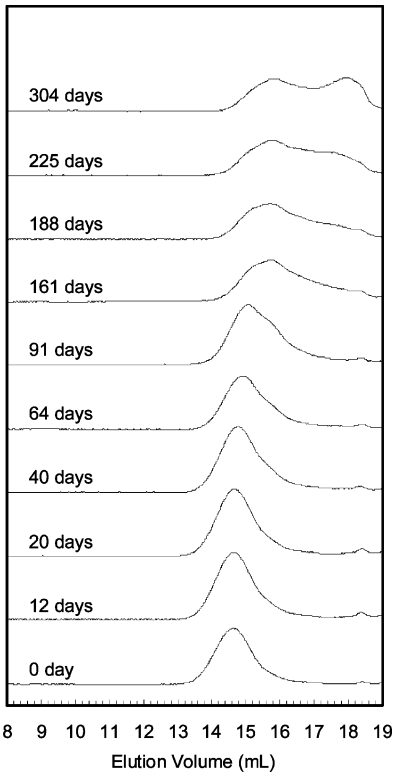

Figure 5. GPC traces of polymandelide samples during hydrolytic degradation at pH = 7.4 and 55 °C.

experiment in several months. The polymandelide samples were ~1 mm solid particles and were aged in phosphate buffer without stirring to simulate the low flow rates of body fluids in smooth and hard tissues.[46]

Weight loss and molecular weight data measured during degradation are given in Table 2. Significant weight loss did not occur until after day 91, while M_n decreased without an induction period. Examination of the GPC traces shows development of a low molecular weight shoulder in samples after 64 days of degradation (Figure 5), which eventually evolved into a well-defined bimodal molecular weight distribution. Molecular weight distributions of this type reflect heterogeneous degradation, and they are often attributed to differences in degradation rates at the polymer surface and in the core.

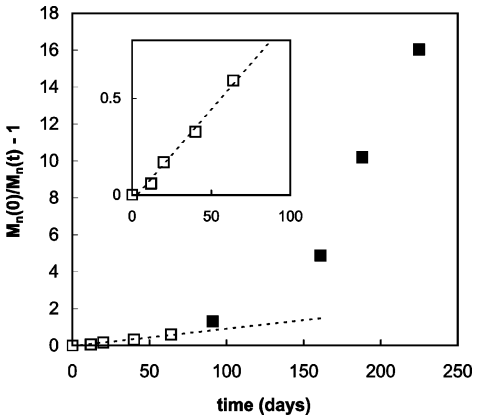

Figure 7. Plot of chain scission as a function of time. The inset shows the linear fit to the first four data points (□).

The two heterogeneous degradation models most often used to describe polylactide degradation are surface erosion and bulk erosion. Tracking the temporal variation of M_n during degradation can discriminate between surface and bulk erosion processes. Surface erosion corresponds to degradation localized in a thin layer at the surface; decrease in M_n and mass loss occur concurrently, but the molecular weight distribution is intrinsically bimodal since degrading samples are comprised of pristine (interior) and degraded chains (surface). In contrast, degradation occurs throughout the sample during bulk erosion, and M_n can decrease without loss of mass. Autocatalysic degradation is another characteristic of bulk erosion. When the conditions of a degradation experiment are below the polymer T_g, hydrolyzed chains cannot diffuse freely through the material, and instead, localized acid groups catalyze hydrolysis of neighboring chains, creating "pockets" where the local acid concentration increases with each chain scission (Figure 6). Consequently, localized autocatalysis also leads to a bimodal distribution in M_n.

The initial stage of bulk erosion is characterized by random chain scission where the average number of cuts per original chain, N, increases linearly with time. As a function of molecular weight, $N(t)$ can be written as $M_n(0)/M_n(t) - 1$, where $M_n(0)$ and $M_n(t)$ are the number-average molecular weights initially and at time t, respectively.[47] Thus, the number of chains as a function of time is given by eq 1, where k is related to chain hydrolysis.[48] Figure 7 shows a plot of eq 1 using the M_n data from Table 2.

Figure 6. Model for heterogeneous degradation in polymandelide. The yellow volumes are regions where chain scission results in autocatalytic hydrolysis.

$$\frac{M_n(0)}{M_n(t)} - 1 = kt \quad (1)$$

The fit to eq 1 is good until $N(t) \geq 1$ (see inset, Figure 7). Beyond this time, the rate of chain scission increases substantially, consistent with autocatalytic hydrolysis by the carboxylic acids generated from chain scission via a bulk degradation mechanism. From the linear portion of the data in Figure 7, we estimate that polymandelide degrades 100 times slower than polylactide under identical conditions.

In addition to supporting a bulk degradation mechanism, the data in Table 2 and the plot in Figure 7 exclude a surface erosion mechanism. Specifically, substantial weight loss should precede a significant decrease in molecular weight if surface erosion were operating. This is because chain scission at the surface would create short, soluble oligomers much faster than hydrolysis would occur in the polymer interior. However, the data in Table 2 clearly show that M_n declines much more rapidly than x. It is also difficult to reconcile the increased rate of hydrolysis that is evident in Figure 7 with a surface erosion mechanism, since any carboxylic acids resulting from hydrolysis at the surface would be immediately neutralized by the phosphate buffer. On the basis of the evidence, the case for degradation via hydrolysis in the polymer interior is reasonably strong.

Bimodal molecular weight distributions were not observed during the degradation of alkyl-substituted polylactides[43] and polyphenyllactide[6] under identical conditions, even though both also degrade by a bulk erosion mechanism. This dichotomy can be attributed to the differences in T_gs between these polymers and polymandelide. The temperature used in the degradation experiments, 55 °C, is higher than the T_g for polylactides and nearly identical to the T_g of polyphenyllactide. Hence, polymer chains in alkyl polylactides and polyphenyllactide samples will have higher mobility at the degradation temperature. High chain mobility will help maintain a homogeneous distribution of acid end groups in the material, giving rise to a decline in M_n that follows the random chain scission model.

The weight loss data also were evaluated for consistency with bulk erosion using the Prout−Tompkins equation[49] (eq 2)

$$\ln(x/(1-x)) + C = kt \quad (2)$$

where x is the mass fraction of polymer that remains, k is the rate of degradation, t is time, and C is a constant. The Prout−Tompkins model applies to solid-state decomposition where the products catalyze the decomposition and has been frequently applied to the degradations of polymers derived from α-hydroxyacids. The correlation between PLA degradation rates and an increase in particle size have been offered as evidence for a bulk degradation mechanism.[50] Figure 8 shows that after an induction period, the fit of the data in Table 2 to eq 2 is reasonably good. For a surface erosion mechanism, x should decay linearly as a function of time, and Figure 8 shows that the fit to this model is only slightly worse. Thus, while the data are consistent with bulk erosion, the Prout−Tompkins analysis of the weight loss data cannot distinguish between the bulk and surface erosion mechanisms.

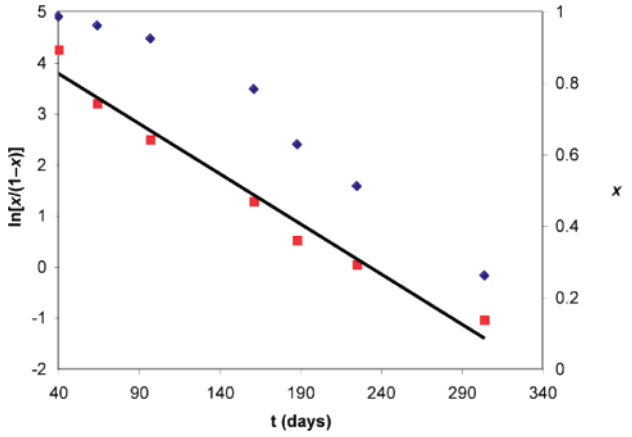

Figure 8. Degradation of polymandelide fit to Prout−Tompkins (■) and surface erosion (◆) models.

Conclusions

A degradable polystyrene mimic was prepared from mandelic acid. Because of facile racemization of the methine proton in mandelide, all polymandelides synthesized were amorphous, clear glassy solids regardless of the initial stereochemistry of the monomer. Hydrolytic degradation at 55 °C proceeds via a bulk erosion mechanism at a rate ∼100 times slower than polylactide under similar conditions. With a T_g comparable to polystyrene and an onset for decomposition near 300 °C, polymandelide captures many of polystyrene's traits in a polymer derived from renewable resources.

Acknowledgment. We thank the Michigan Economic Development Corp. and the Center for Fundamental Materials Research for partial support of this work.

Supporting Information Available: Data showing establishment of an equilibrium monomer pool in solution polymerizations and ^{13}C NMR spectra of polymandelide. This material is available free of charge via the Internet at http://pubs.acs.org.

References and Notes

(1) Stridsberg, K. M.; Ryner, M.; Albertsson, A. C. *Adv. Polym. Sci.* **2002**, *157*, 41.
(2) Chiellini, E.; Solaro, R. *Adv. Mater.* **1996**, *8*, 305−313.
(3) Auras, R.; Harte, B.; Selke, S. *Macromol. Biosci.* **2004**, *4*, 835.
(4) Duda, A.; Penczek, S. *Polimery* **2003**, *48*, 16.
(5) Thayer, A. *Chem. Eng. News* **1997**, *75*, 14−16.
(6) Simmons, T. L.; Baker, G. L. *Biomacromolecules* **2001**, *2*, 658.
(7) Pinkus, A. G.; Subramanyam, R.; Clough, S. L.; Lairmore, T. C. *J. Polym. Sci., Part A: Polym. Chem.* **1989**, *27*, 4291−4296.
(8) Domb, A. J. *J. Polym. Sci., Part A: Polym. Chem.* **1993**, *31*, 1973−1981.
(9) Okada, T.; Okawara, R. *J. Organomet. Chem.* **1973**, *54*, 149−152.
(10) Kobayashi, S.; Yokoyama, T.; Kawabe, K.; Saegusa, T. *Polym. Bull. (Berlin)* **1980**, *3*, 585−591.
(11) Smith, I. J.; Tighe, B. J. *Macromol. Chem. Phys.* **1981**, *182*, 313−324.
(12) Fukuzaki, H.; Aiba, Y.; Yoshida, M.; Asano, M.; Kumakura, M. *Macromol. Chem. Phys.* **1989**, *190*, 2407.
(13) Fukuzaki, H.; Yoshida, M.; Asano, M.; Kumakura, M.; Imasaka, K.; Nagai, T.; Mashimo, T.; Yuasa, H.; Imai, K.; Yamanaka, H. *Eur. Polym. J.* **1990**, *26*, 1273−1277.
(14) Imasaka, K.; Nagai, T.; Yoshida, M.; Fukuzaki, H.; Asano, M.; Kumakura, M. *Macromol. Chem. Phys.* **1990**, *191*, 2077−2082.
(15) Imasaka, K.; Yoshida, M.; Fukuzaki, H.; Asano, M.; Kumakura, M.; Mashimo, T.; Yamanaka, H.; Nagai, T. *Int. J. Pharm.* **1992**, *81*, 31−38.
(16) Whitesell, J. K.; Pojman, J. A. *Chem. Mater.* **1990**, *2*, 248−254.
(17) Kylma, J.; Harkonen, M.; Seppala, J. V. *J. Appl. Polym. Sci.* **1997**, *63*, 1865−1872.
(18) Moon, S. I.; Urayama, H.; Kimura, Y. *Macromol. Biosci.* **2003**, *3*, 301.
(19) Kowalski, A.; Libiszowski, J.; Duda, A.; Penczek, S. *Macromolecules* **2000**, *33*, 1964−1971.
(20) Leemhuis, M.; van Nostrum, C. F.; Kruijtzer, J. A. W.; Zhong, Z. Y.; ten Breteler, M. R.; Dijkstra, P. J.; Feijen, J.; Hennink, W. E. *Macromolecules* **2006**, *39*, 3500−3508.
(21) Gerhardt, W. W.; Noga, D. E.; Hardcastle, K. I.; Garcia, A. J.; Collard, D. M.; Weck, M. *Biomacromolecules* **2006**, *7*, 1735.
(22) Trimaille, T.; Moller, M.; Gurny, R. *J. Polym. Sci., Polym. Chem.* **2004**, *42*, 4379.
(23) Duda, A.; Penczek, S. *Macromolecules* **1990**, *23*, 1636−1639.

(24) Witzke, D. R.; Narayan, R.; Kolstad, J. J. *Macromolecules* **1997**, *30*, 7075−7085.
(25) Whitesell, J. K.; Reynolds, D. *J. Org. Chem.* **1983**, *48*, 3548−3551.
(26) Schoberl, A.; Wiehler, G. *Ann. Chem.* **1955**, *595*, 101−130.
(27) Lomellini, P. *Polymer* **1992**, *33*, 1255.
(28) Racemization is slow in the absence of the Sn(2-ethylhexanoate)$_2$ catalyst under the same conditions.
(29) Fox, T. G.; Flory, P. J. *J. Polym. Sci.* **1954**, *14*, 315.
(30) Fox, T. G.; Flory, P. J. *J. Am. Chem. Soc.* **1948**, *70*, 2384.
(31) Graessley, W. W. *J. Polym. Sci., Part B: Polym. Phys.* **1980**, *18*, 27.
(32) Cheng, M.; Attygalle, A. B.; Lobkovsky, E. B.; Coates, G. W. *J. Am. Chem. Soc.* **1999**, *121*, 11583−11584.
(33) Ovitt, T. M.; Coates, G. W. *J. Am. Chem. Soc.* **1999**, *121*, 4072−4073.
(34) Spassky, N.; Pluta, C.; Simic, V.; Thiam, M.; Wisniewski, M. *Macromol. Symp.* **1998**, *128*, 39−51.
(35) Spassky, N.; Wisniewski, M.; Pluta, C.; LeBorgne, A. *Macromol. Chem. Phys.* **1996**, *197*, 2627−2637.
(36) Bero, M.; Dobrzynski, P.; Kasperczyk, J. *J. Polym. Sci., Polym. Chem.* **1999**, *37*, 4038−4042.
(37) Qian, B., unpublished work.
(38) Chuchani, G.; Martin, I. *J. Phys. Org. Chem.* **1997**, *10*, 121−124.
(39) Chuchani, G.; Rotinov, A.; Dominguez, R. M.; Martin, I. *J. Phys. Org. Chem.* **1996**, *9*, 348−354.
(40) Chuchani, G.; Dominguez, R. M.; Herize, A.; Romero, R. *J. Phys. Org. Chem.* **2000**, *13*, 757−764.
(41) The ratio of decomposition rates of acetyllactic acid and lactic acid at 200 °C is 78:1. This provides a scaling factor for estimating the decomposition of the polymer relative to the rate for the corresponding α-hydroxy acid. The estimate for the gas phase decomposition rate from the scaling factor and the extrapolated decomposition rate for mandelic acid at 200 °C is $k \approx 4.6 \times 10^{-7}$ s^{-1}.
(42) Polymandelide might also degrade faster than polylactide if hydrogen atom abstraction contributes to decomposition. In the absence of a radical initiator, we would not expect this to be important on the basis of Chuchani's gas phase decomposition studies.
(43) Yin, M.; Baker, G. L. *Macromolecules* **1999**, *32*, 7711−7718.
(44) Matsusue, Y.; Yamamuro, T.; Oka, M.; Shikinami, Y.; Hyon, S. H.; Ikada, Y. *J. Biomed. Mater. Res.* **1992**, *26*, 1553−1567.
(45) Therin, M.; Christel, P.; Li, S. M.; Garreau, H.; Vert, M. *Biomaterials* **1992**, *13*, 594−600.
(46) Li, S. *J. Biomed. Mater. Res.* **1999**, *48*, 342−353.
(47) Seki, T.; Ichimura, K. *Macromolecules* **1990**, *23*, 31−35.
(48) Specifically, $k = k_{hyd}X_n(0)$, where k_{hyd} is the hydrolysis rate constant and $X_n(0)$ is the number-average degree of polymerization at time zero.
(49) Brown, M. E.; Glass, B. D. *Int. J. Pharm.* **1999**, *190*, 129.
(50) Grizzi, I.; Garreau, H.; Li, S.; Vert, M. *Biomaterials* **1995**, *16*, 305−311.

MA061839N